

# Direct Assembly of Magnetic Janus Particles at a Droplet Interface

Qingguang Xie,<sup>1</sup> Gary B. Davies,<sup>2</sup> and Jens Harting<sup>\*,3,1</sup>

<sup>1</sup>*Department of Applied Physics, Eindhoven University of Technology,  
P.O. Box 513, 5600MB Eindhoven, The Netherlands*

<sup>2</sup>*St Paul's Girls' School, Brook Green, Hammersmith, London W6 7BS, United Kingdom*

<sup>3</sup>*Forschungszentrum Jülich, Helmholtz Institute Erlangen-Nürnberg for  
Renewable Energy (IEK-11), Fürther Straße 248, 90429 Nürnberg, Germany.*

<sup>\*</sup>*j.harting@fz-juelich.de*

**ABSTRACT:** Self-assembly of nanoparticles at fluid-fluid interfaces is a promising route to fabricate functional materials from the bottom-up. However, directing and controlling particles into highly tunable and predictable structures – while essential – is a challenge. We present a liquid interface assisted approach to fabricate nanoparticle structures with tunable properties. To demonstrate its feasibility, we study magnetic Janus particles adsorbed at the interface of a spherical droplet placed on a substrate. With an external magnetic field turned on, a single particle moves to the location where its position vector relative to the droplet centre is parallel to the direction of the applied field. Multiple magnetic Janus particles arrange into reconfigurable hexagonal lattice structures and can be directed to assemble at desirable locations on the droplet interface by simply varying the magnetic field direction. We develop an interface energy model to explain our observations, finding excellent agreement. Finally, we demonstrate that the external magnetic field allows one to tune the particle deposition pattern obtained when the droplet evaporates. Our results have implications for the fabrication of varied nanostructures on substrates for use in nanodevices, organic electronics, or advanced display, printing and coating applications.

**Keywords:** Janus particles, direct assembly, tunable deposition, colloids at interfaces, advanced printing techniques

The self-assembly of nanoparticles provides a promising route to fabricate nano- and microstructured functional materials.<sup>1</sup> In this type of self-assembly, the particles organise into interesting structures due to particle-particle interactions such as molecular bonds,<sup>2</sup> electromagnetic interactions,<sup>3</sup> and capillary interactions. For technological applications, we need the ability to direct and control the particles so that they assemble into desirable structures, and this ability remains one of the biggest challenges in nanoscience.<sup>4,5</sup>

Fluid-fluid interfaces have been identified as a promising platform for the controllable assembly of nanoparticles. Nanoparticles trap irreversibly at fluid interfaces because they reduce the area of the energetically-costly interface, and once absorbed, they try to arrange into their lowest energy configurations.<sup>6,7</sup> For example, spherical CdSe nanoparticles assemble into a disordered but densely packed monolayer to reduce the total interfacial energy.<sup>7</sup> Moreover, going beyond the canonical case of spherical particles with uniform surface properties to particles that exhibit anisotropy (*e.g.*, ellipsoids, rods) and non-uniform surface properties (*e.g.*, Janus-like particles) provides more varied behaviour. For example, nanorods can be used to generate different packing structures simply by varying their aspect ratio.<sup>8</sup> However, until recently<sup>5,9</sup> it has been difficult to direct and control the assembly process since the arrangements of particles depended only on the intrinsic properties of the particles and interfaces and not on properties that can be controlled on-the-fly.

The synthesis of anisotropic particles with specific

physical properties (*e.g.*, electric or magnetic moments) that interact with an external magnetic or electric field allows greater control of the self-assembly process at fluid interfaces because we can easily vary the external field: the interfacial energy of anisotropic particles at a fluid-fluid interface depends on their orientation<sup>10–13</sup> and the external field can be used to change the orientation of the particles. Recently, Davies *et al.*<sup>14</sup> investigated the behaviour of magnetic ellipsoidal particles at flat fluid-fluid interfaces, and they demonstrated that the capillary interactions between magnetic ellipsoidal particles can be tuned by varying an external magnetic field, resulting in switchable, network-like monolayer structures. Similarly, Xie *et al.*<sup>15</sup> showed that spherical magnetic Janus particles adsorbed at flat fluid-fluid interfaces can generate highly ordered, chain-like structures that can be controlled by altering an external magnetic field.

Most research to date, however, has focussed on the behaviour of these particles at flat fluid-fluid interfaces, a situation that is quite artificial in the real world where most fluid-fluid interfaces exhibit some degree of curvature. More recently, particles at curved fluid-fluid interfaces were used to show interesting phenomena. Cavallaro *et al.*<sup>16</sup> demonstrated that on a curved fluid interface, rod-like particles move to areas of greatest curvature due to the interaction between particle induced deformation and the natural curvature gradient of the interfaces. Ershov *et al.*<sup>17</sup> showed that isotropic colloids organise into a square pattern aligned along the principle curvature axis of a curved interface. However, the interface curvature driven assembly approach investigated to date relies on

having quite complex control of the interface curvature, and is therefore less relevant to the situation where particles assemble at an isotropically-curved fluid interface, such as a spherical droplet interface.

In this paper, we study the behaviour of spherical magnetic Janus particles adsorbed at a spherical droplet interface interacting with an external magnetic field. We show that we are able to direct the location of particles by varying the magnetic field direction on this isotropically curved interface and exploit the anisotropic surface properties of Janus particles. We demonstrate that the particles assemble into a highly ordered hexagonal lattice-like monolayer at a spherical droplet interface, which is drastically different from the structures formed at a flat fluid-fluid interface.<sup>15</sup> Moreover, we demonstrate that by changing the direction of the magnetic field, it is possible to tune the particle deposition pattern during the evaporation of a Janus particle-laden droplet, thus providing a controllable platform for the fabrication of desirable nanostructures on substrates for various nanodevices.

## RESULTS AND DISCUSSION

**Geometry and surface properties.** In order to understand the behaviour of multiple Janus particles adsorbed at a surface droplet interface during evaporation, we first study the behaviour of a single Janus particle. Fig. 1 illustrates the system, which comprises of a spherical magnetic Janus particle of radius  $a$  adsorbed at the interface of a droplet deposited on a chemically patterned substrate. The substrate covered by the droplet is hydrophilic with contact angle  $30^\circ$  and the rest of the substrate is hydrophobic with contact angle  $120^\circ$ . Thus, the droplet will be confined to the hydrophilic area with an effective contact angle, and for simplicity we limit ourselves to investigating a droplet of radius  $R$  with an initial contact angle of  $90^\circ$ . We consider the case of low Bond numbers in which the effect of gravity of the fluids is negligible and the system is surface tension dominated, thus, the droplet has a spherical shape with its centre located at  $O$ , as shown in Fig. 1a.

The Janus particle comprises an apolar and a polar hemisphere with opposite wettability, defined by the three-phase contact angles  $\theta_A = 90^\circ + \beta$  and  $\theta_P = 90^\circ - \beta$ , respectively, where  $\beta$  represents the amphiphilicity of the particle. The boundary between these two hemispheres is called the Janus boundary. The particle's magnetic dipole moment  $\mathbf{m}$  is orthogonal to the Janus boundary, and the applied external magnetic field is denoted by  $\mathbf{H}$ . We define a dipole-field strength  $B_m = |\mathbf{m}||\mathbf{H}|$ , which represents the magnitude of the interaction between the magnetic dipole and the external magnetic field. The angle between the particle's magnetic dipole vector and the horizontal axis is denoted by  $\alpha$ . We define a droplet field vector  $\mathbf{r}_0$  beginning at the droplet centre  $O$  and ending at the droplet interface that is directed parallel to the external magnetic field. We further define a particle position

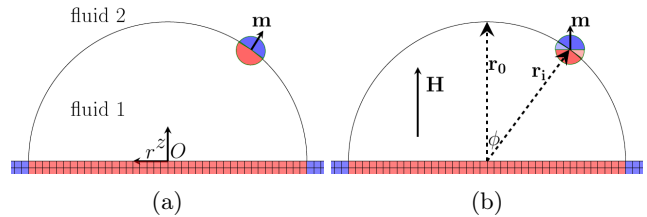


FIG. 1: Side views of a single Janus particle adsorbed at a droplet interface in its equilibrium orientation (a) and under the influence of a vertical magnetic field (b). The

Janus particle comprises an apolar and a polar hemisphere. The particle's magnetic dipole moment  $\mathbf{m}$  is orthogonal to the Janus boundary, and the external magnetic field,  $\mathbf{H}$ , is directed vertically upward. The angle  $\phi$  is defined as the angle between vector  $\mathbf{r}_0$  and particle position vector  $\mathbf{r}_i$ .

vector  $\mathbf{r}_i$  that points from the droplet centre  $O$  to the particle centre. Finally, the angle  $\phi$  is defined as the angle between droplet field vector  $\mathbf{r}_0$  and particle position vector  $\mathbf{r}_i$ .

In its equilibrium state, the two hemispheres of the Janus particle are fully immersed in their preferred fluid, as shown in Fig. 1a. After switching on an upward magnetic field,  $\mathbf{H}$ , the particle experiences a magnetic torque that aligns it instantly with the dipole axis parallel to the field, as shown in Fig. 1b.

### Single magnetic Janus particle.

To simulate the behaviour of the Janus particle adsorbed at the droplet interface, we use a lattice Boltzmann method combined with a molecular dynamics algorithm that has been developed and validated extensively in previous research projects,<sup>12,15,18–21</sup> which we briefly summarise in the Methods section. Initially, we place a particle at the droplet interface with fixed orientation  $\alpha = 23.6^\circ$  vertically located at  $z = 0.4R$  and let the system equilibrate. After equilibration, we release the particle and simultaneously switch on an upward magnetic field.

Fig. 2 shows time evolution of the vertical position  $z$  for particles with different amphiphilicities and dipole-field strengths  $B_m/\pi a^2 \gamma_{12} = 1.31$ . The time is normalized by the viscosity of the fluid  $\mu$ , particle radius  $a$ , and surface tension  $\gamma_{12}$ . For all amphiphilicities, the particle experiences a quick acceleration and moves upward. When the particle approaches the top of the droplet, it slows down and finally remains at the droplet's top ( $\phi = 0$ ). Moreover, we observe that particles with larger amphiphilicities  $\beta$  move faster just after the magnetic field is applied. This observation cannot be explained by theories that suggest particles to move to areas of highest curvature<sup>17</sup> since the curvature of a spherical droplet interface is isotropic.

To understand these observations, we develop a model describing the interface energy of this system assum-

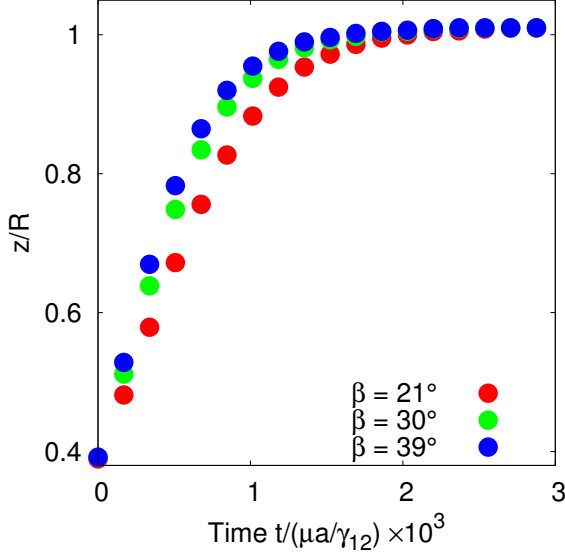


FIG. 2: Time evolution of vertical position  $z$  for particles with different amphiphilicities  $\beta = 21^\circ$  (red),  $\beta = 30^\circ$  (cyan) and  $\beta = 39^\circ$  (blue).

ing that (i) the interface deformation caused by the nanometer-sized Janus particle is negligible,<sup>10</sup> (ii) and that the particle radius is substantially smaller than the droplet radius. To derive our model, we compare the interface energy for the particle in its equilibrium state adsorbed on the droplet interface with its energy under the influence of an external magnetic field.

The interface energy for a particle in its equilibrium state (Fig. 1a) is

$$E_{\text{int}} = \gamma_{12}A_{12}^{\text{int}} + \gamma_{a1}A_{a1}^{\text{int}} + \gamma_{p2}A_{p2}^{\text{int}}. \quad (1)$$

Here,  $\gamma_{ij}$  are the interface tensions between phases  $i$  and  $j$  and  $A_{ij}$  are the contact surface areas between phases  $i$  and  $j$ , where  $i, j = \{1: \text{fluid}, 2: \text{fluid}, a: \text{apolar}, p: \text{polar}\}$ . The interface energy for a particle in an external magnetic field (Fig. 1b) is

$$E_{\text{mag}} = \gamma_{12}A_{12}^{\text{mag}} + \gamma_{a1}A_{a1}^{\text{mag}} + \gamma_{p2}A_{p2}^{\text{mag}} + \gamma_{a2}A_{a2} + \gamma_{p1}A_{p1}. \quad (2)$$

The interface energy difference between the magnetic field induced orientation state and the initial equilibrium state is

$$\Delta E = 4\phi a^2 \gamma_{12} \sin \beta. \quad (3)$$

The detailed introduction to this model is presented in the Methods section.

The interaction energy  $\Delta E$  in Eq. (3) is proportional to the particle position angle  $\phi$ . Thus, minimising the interface energy requires that the particle moves to the top of the droplet where  $\phi = 0$ , in agreement with our simulation results. Our theoretical model also predicts that

particles with larger amphiphilicities cause a larger interface energy jump, explaining why the particle with higher amphiphilicity moves faster to the top of the droplet, as observed in our simulations.

We note that the magnetic Janus particles will relocate when we vary the direction of the magnetic field, which has potential applications in sensor or display technology. To estimate the responsive time of the magnetic Janus particles, we assume that a nanoparticle with radius  $a = 10 \text{ nm}$  is adsorbed at an oil-water droplet interface of radius  $R = 100 \text{ nm}$ , with surface tension  $\gamma_{12} = 70 \text{ mN/m}$ , and viscosity  $\mu = 1.0 \text{ mPa} \cdot \text{s}$ .<sup>22,23</sup> Based on our simulation results shown in Fig. 2, the normalized time  $t/(\mu a/\gamma_{12})$  needed for the particle to relocate to the droplet top is  $\approx 3 \times 10^3$ . Therefore, the estimated response time is around  $(\mu a/\gamma_{12}) \times 3 \times 10^3 \approx 4 \times 10^{-7} \text{ s} \approx 400 \text{ ns}$ , which is fast enough to satisfy the requirements of responsive materials for advanced sensor or display technology.<sup>24</sup> For a possible experimental realization of our system, we note that surface nanodroplets can be produced through a solvent exchange process in experiments.<sup>25,26</sup>

**Multiple magnetic Janus particles.** Having obtained a good understanding of the behaviour of a single magnetic Janus particle adsorbed at a surface droplet interface, we investigate the self-assembly of multiple magnetic Janus particles. Starting from a random initial placement of 3 magnetic Janus particles adsorbed at the interface, we let the system reach the steady-state. We then add one more particle at the droplet interface, let the system reach steady state again and repeat this process for up to  $N = 6$  particles. We show the structures obtained in Fig. 3 for a given number of particles.

$N = 3$  particles arrange into a triangular lattice-like structure around the droplet centre (Fig. 3a), instead of the straight chain-like configuration found by magnetic Janus particles at flat fluid-fluid interfaces.<sup>15</sup> This structure is similar to the 3-particle structure observed for colloidal particles adsorbed at a liquid crystal droplet interface<sup>27</sup> and for colloidal particles interacting with short range-interactions.<sup>28,29</sup> For  $N = 4 - 6$  particles, we find the particles all favour hexagonal arrangements (Fig. 3b, Fig. 3c and Fig. 3d), which suggests the hexagonal arrangement may be the interface energy minimum configuration for  $N > 3$  particles.

Applying our free energy model for a single particle to the case for  $N$  particles with assuming that the magnetic dipole-dipole interactions between the particles are negligible, the interface energy is:

$$\Delta E_t = 4a^2 \gamma_{12} \sin \beta \sum_i^N \phi_i. \quad (4)$$

To estimate the total interface energy for the 3-particle system, we fix two particles next to each other, and move the third particle with the pair angle  $\varphi$  from  $\varphi = 0^\circ$  to  $\varphi = 120^\circ$ , as illustrated in the inset of Fig. 4. Fig. 4 shows that the interface energy decreases monotonically with

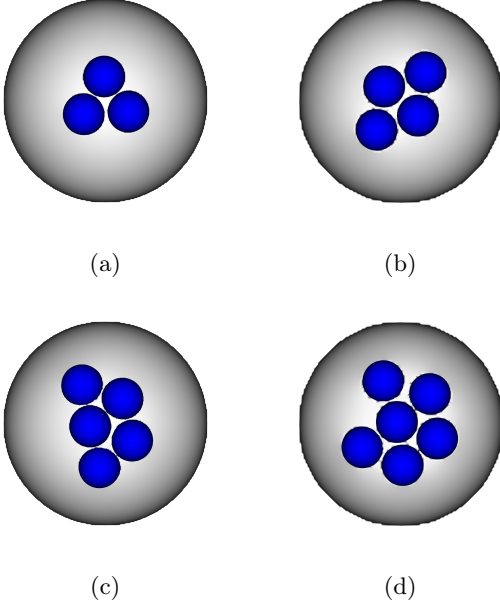


FIG. 3: Clusters observed in simulations for  $N = 3 - 6$  particles with amphiphilicity  $\beta = 30^\circ$  and external dipole-field strength  $B_m/\pi a^2 \gamma_{12} = 1.31$ . The particles exhibit a hexagonal lattice-like arrangement.

increasing particle pair-pair angle  $\varphi$  and the interface energy becomes minimal at  $\varphi = 120^\circ$ , which represents a triangular arrangement, in agreement with simulation results.

For  $N = 4 - 6$  particles, it is nontrivial to estimate the interface energy as a function of a single parameter, however, after some mathematical analysis we find that minimising  $\sum_i^N \phi_i$  is identical to minimising the total particle-centre to droplet-centre distance  $L = \sum_i^N |\mathbf{r}_i - \mathbf{r}_0|$ , with the following two constraints: 1) particles are located at the droplet interface,  $|\mathbf{r}_i| = R$ , and 2) particles do not overlap,  $|\mathbf{r}_i - \mathbf{r}_j| \geq 2a$ . In addition, in a strong magnetic field, the orientation of the particle is fixed parallel to the magnetic field direction and the particles are adsorbed at the droplet interface, which leaves only two degrees of freedom for the particles. Therefore, we can model our system as a quasi-2D system. Minimising  $L$  for spherical particles in a 2D system yields particles that conform to closest packing, which is a hexagonal arrangement. Therefore, our theoretical model's prediction that hexagonal arrangement is energetically favourable for self-assembly of multiple magnetic Janus particles agrees with our simulation results.

**Varying the magnetic field direction.** With even more particles  $N = 40$ , we investigate the relocation and rearrangement of particles by varying the external field starting from pointing vertically upward, to vertically downward and finally to left horizontal direction. Under an upward magnetic field, the particles assemble

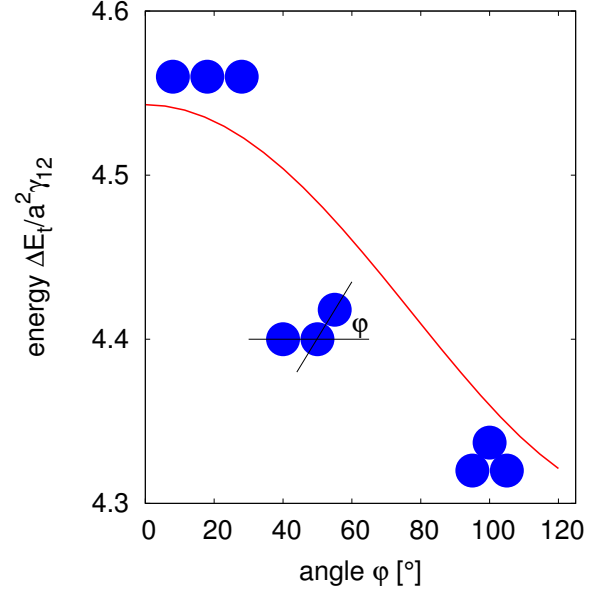


FIG. 4: Normalized interface energy  $\Delta E_t/a^2 \gamma_{12}$  as a function of particle pair-pair angle  $\varphi$ . The interface energy takes a minimum at  $\varphi = 120^\circ$ , which represents a triangular lattice-like arrangement, in agreement with our simulation results.

at the top of the droplet ordered in a hexagonal arrangement (Fig. ?? and Fig. ??). When we switch the magnetic field to the downward direction, the particles rotate instantly by  $180^\circ$ , move immediately downwards towards the surface droplet contact line and finally align in a ring-like structure at the edge of the droplet (Fig. ?? and Fig. ??). On switching the magnetic field to the left horizontal direction, the particles rotate by  $90^\circ$ , move to the left side of the droplet and form highly ordered layers (Fig. ?? and Fig. ??). [Movie S1]

Our simulations therefore show that it is possible to direct the particles to assemble at desirable locations at the droplet interface based on the direction of the external magnetic field, and that the final assembled structure is tunable depending on the direction and magnitude of the applied magnetic field. One can immediately foresee technological applications as *e.g.*, a photonic material or alternative to currently used electrophoretic/electronic inks (E-inks), where electrophoretic particles encapsulated in a microdroplet are relocated by an external electric field.<sup>30</sup>

**Particle deposition during evaporation.** Finally, we investigate the case of many magnetic Janus particles adsorbed at a surface droplet interface that undergoes evaporation, a scenario that occurs frequently in reality when coatings and paints dry. To simulate fluid evaporation, we use a diffusion dominated evaporation model, developed recently in our group.<sup>18</sup> The starting configuration of the system before evaporation is the same as those shown in *e.g.*, Fig 5. Once a steady-state is reached,

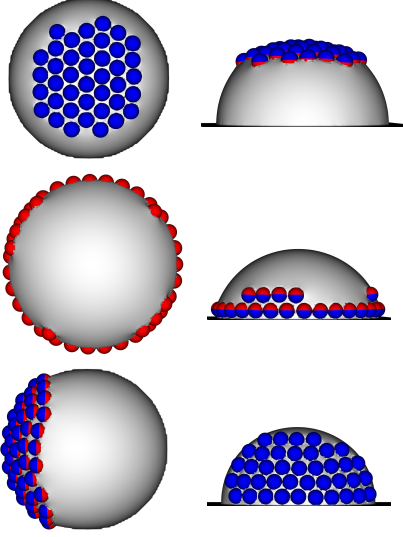


FIG. 5: Snapshot of  $N = 40$  particles adsorbed at a droplet interface with amphiphilicity  $\beta = 30^\circ$  and dipole-field strength  $B_m / \pi a^2 \gamma_{12} = 1.31$  under different magnetic field directions. The particles relocate and form different ordered structures depending on the direction of the magnetic field.

we start to evaporate the droplet.

When an upward magnetic field is applied, the particles stay at the top during the evaporation of the droplet (Fig. ??). The contact angle of the droplet decreases until it reaches  $30^\circ$ , after which the contact lines de-pin from the border of the hydrophilic area and moves towards the centre (Fig. ??). This is the well-known stick-slip phenomenon,<sup>25</sup> usually encountered during the evaporation of droplets on a rough solid substrate. After the contact line depins, the droplet continues to dewet (Fig. ??) and approaches the geometry of a planar film. The Janus particle will deform the planar film in a monopolar fashion, introducing attractive capillary forces between particles. The attractive capillary forces ensure close packing of the particles, and finally, a dried highly ordered particle monolayer remains on the substrate (Fig. ??). [Movie S2]

Under the influence of a downward magnetic field, the particles stay at the edge of the droplet, forming a ring-like structure during the evaporation of droplet (Fig. ??). The contact angle of the droplet continuously decreases. We do not observe depinning behaviour once the contact angle reaches  $30^\circ$ , in contrast with the behaviour observed for an upwardly directed magnetic field. This is caused by self-pinning due to the particles confined at the contact line. The colloidal particles experience friction with the substrate, thus strengthening the pinning of the contact line on the substrate. When the contact angle decreases further approaching zero degrees, the liquid film begins to rupture at areas on the edge of the droplet (Fig. ??) and the droplet rapidly dries in these areas (Fig. ??). Finally, after full evaporation, a ring-like

particle structure is deposited on the substrate (Fig. ??). [Movie S3]

Under a left oriented horizontal magnetic field, the particles stay at the left side of the droplet during the evaporation, as naively expected (Fig. ??). The contact angle of the droplet continuously decreases, and the contact line depins first at the right side where there is no self-pinning due to the Janus particles (Fig. ??). The contact angle approaches zero degrees and the droplet geometry tends to that of a planar film, similar to the case of an upwardly directed magnetic field. In contrast with the upwardly directed magnetic field, under a horizontal magnetic field, the Janus particles deform the planar film in a dipolar fashion<sup>12,15</sup>, and dipolar capillary interactions arise (Fig. ??). This dipolar capillary force is repulsive between neighbouring particles in the horizontal direction<sup>15</sup>, thus the final structure shows a looser arrangement of particles (Fig. ??) compared with the particle deposition formed in an upward magnetic field (Fig. ??). [Movie S4]

Our results demonstrate that the direction of the magnetic field allows one to tune the particle deposition pattern obtained due to the evaporation and drying of a Janus particle-laden droplet, which can find potential applications in e.g. advanced printing, electronics or display

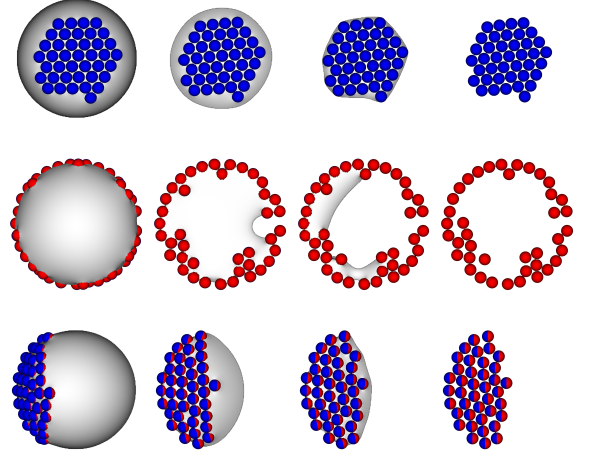


FIG. 6: Snapshots of the assembled structures during droplet evaporation and with an upward (a)-(d), downward (e)-(h) and left horizontal (i)-(l) applied magnetic field. Influenced by an upward magnetic field (a-d), the particles remain at the top of the droplet while the contact line decreases before it de-pins. Under a downward magnetic field (e-h), the particles form a ring-like structure that self-pins the contact line, and the contact line decreases continuously. Finally, in a horizontal magnetic field (i-l) the particles migrate in the field direction and cause self-pinning on one side of the droplet, while the contact line recedes on the opposite side and causes inhomogeneous evaporation leading to looser particle arrangements.



technology.

## CONCLUSION

We investigated the behaviour of magnetic Janus particles at a surface droplet interface interacting with an external magnetic field and showed that it is drastically different from the behaviour of such particles adsorbed at a flat fluid-fluid interface. We found that the particles move to the location where the particle position vector is parallel to the direction of applied the field. When multiple Janus particles adsorb at the interface, the particles arrange hexagonally in contrast to the straight chains observed for magnetic Janus particles at a flat interface.<sup>15</sup> We developed an interface free energy model describing this system, and found that our model predicts the behaviour observed in our simulations.

Finally, we investigated the behaviour of magnetic Janus particles adsorbed at a surface droplet interface that undergoes evaporation, finding interesting behaviour at the contact line. In addition, we showed that it is possible to tune the deposition of the particles by varying the magnetic field direction during evaporation.

Our results describe a possible way of creating highly ordered and – more importantly – tunable structures for hierarchical materials assembly. Possible applications are ubiquitous not only in the bottom up formulation of nanostructured surfaces and materials, but also where the ease of reconfiguration by applying an external magnetic field is of advantage: The fast response time of magnetic Janus nanoparticles together with their tunable collective behaviour have implications for advanced display, E-ink, and sensor technologies.

## METHODS

**Simulation method.** We use the lattice Boltzmann method (LBM) for the simulation of fluids. The LBM can be treated as an alternative solver for the Navier-Stokes equations in the limit of low Knudsen and Mach numbers and has gained popularity due to its straightforward implementation. The locality of the algorithm allows for efficient parallelization.<sup>31</sup> The method's popularity also stems from the variety of multiphase/ multicomponent extensions<sup>32,33</sup> and the ability to simulate suspensions.<sup>34</sup> We utilize the pseudopotential multicomponent LBM model, developed by Shan and Chen<sup>32</sup> and present some relevant details in the following. Two fluid components are modelled by following the evolution of the single-particle distribution function discretized in space and time,

$$f_i^c(\mathbf{x} + \mathbf{c}_i \Delta t, t + \Delta t) = f_i^c(\mathbf{x}, t) + \Omega_i^c(\mathbf{x}, t), \quad (5)$$

where  $i = 1, \dots, 19$ .  $f_i^c(\mathbf{x}, t)$  are the single-particle distribution functions for fluid component  $c = 1$  or  $2$ ,  $\mathbf{c}_i$  is the

discrete velocity in the  $i$ th direction, and

$$\Omega_i^c(\mathbf{x}, t) = -\frac{f_i^c(\mathbf{x}, t) - f_i^{\text{eq}}(\rho^c(\mathbf{x}, t), \mathbf{u}^c(\mathbf{x}, t))}{(\tau^c / \Delta t)} \quad (6)$$

is the Bhatnagar-Gross-Krook (BGK) collision operator.<sup>35</sup> Here,  $f_i^{\text{eq}}(\rho^c(\mathbf{x}, t), \mathbf{u}^c(\mathbf{x}, t))$  is a third-order equilibrium distribution function.<sup>36</sup>  $\tau^c$  is the relaxation time of component  $c$ , which determines the speed of relaxation of the distribution function towards the equilibrium. The macroscopic densities and velocities are given as  $\rho^c(\mathbf{x}, t) = \rho_0 \sum_i f_i^c(\mathbf{x}, t)$ , where  $\rho_0$  is a reference density, and  $\mathbf{u}^c(\mathbf{x}, t) = \sum_i f_i^c(\mathbf{x}, t) \mathbf{c}_i / \rho^c(\mathbf{x}, t)$ , respectively. For simplicity, We choose the lattice constant  $\Delta x$ , the timestep  $\Delta t$ , the unit mass  $\rho_0$  and the relaxation time  $\tau^c$  to be unity throughout this paper.

Shan and Chen introduced a pseudopotential interaction between fluid components  $c$  and  $c'$ . A sufficiently strong interaction parameter ( $g^{cc'}=0.1$  in our case) triggers the separation of components and the formation of a diffuse interface with a well defined surface tension. The typical width of this interface is  $\approx 5\Delta x$ .<sup>32</sup> The components separate into a denser majority phase of density  $\rho_{ma}$  and a lighter minority phase of density  $\rho_{mi}$ , respectively. In order to simulate evaporation, we impose the density of component  $c$  at the boundary sites to be a constant value.<sup>18</sup> In addition, we apply Shan-Chen type potentials between solid walls and the fluid<sup>37</sup> in order to tune the wettability of the substrate.

To model the particles, we discretize them on the fluid lattice and couple them to the fluid species by means of a modified bounce-back boundary condition as pioneered by Ladd and Aidun.<sup>34,38</sup> Lubrication forces between particles are properly resolved by the LBM until a distance of one  $\Delta x$  between the particle surfaces. If particles get closer, we add a short-range lubrication correction<sup>34</sup> as well as a Hertz force between the particles.<sup>19</sup> The method was later extended to multiphase flows.<sup>19,39,40</sup>

For particles with magnetic dipole moment  $\mathbf{m}$ , the dipole-dipole interaction is

$$U_{ij} = \frac{\mu_0}{4\pi} \frac{m_i m_j}{r_{ij}^3} [\hat{\mathbf{o}}_i \cdot \hat{\mathbf{o}}_j - 3(\hat{\mathbf{o}}_i \cdot \hat{\mathbf{r}}_{ij})(\hat{\mathbf{o}}_j \cdot \hat{\mathbf{r}}_{ij})], \quad (7)$$

where  $\mu_0 = 4\pi \times 10^{-7}$  is the magnetic constant,  $\hat{\mathbf{o}}$  is the unit vector of the orientation of the particle,  $r_{ij}$  is the distance between particle  $i$  and  $j$ ,  $\hat{\mathbf{r}}_{ij} = \frac{\mathbf{r}_i - \mathbf{r}_j}{|\mathbf{r}_i - \mathbf{r}_j|}$  and  $m_i$  is the magnitude of the magnetic dipole in particle  $i$ . The dipole-dipole interaction force is  $F_{dd} \approx \frac{\mu_0}{4\pi} \frac{m_i m_j}{r_{ij}^3}$ .

A magnetic dipole in an external magnetic field  $\mathbf{H}$  experiences a force  $F_i = m_i \hat{\mathbf{o}}_i \cdot \Delta \mathbf{H}$ , and a torque  $T_i = m_i \hat{\mathbf{o}}_i \times \mathbf{H}$ . In our simulations, we set the dipole moment  $|\mathbf{m}| = 1$ , the magnetic field  $|\mathbf{H}| = 20$ , and the particle radius  $a = 10$  or  $a = 20$ . Thus, the dipole-dipole interaction force  $F_{dd} \approx \frac{\mu_0}{4\pi} \frac{m_i m_j}{r_{ij}^3}$  is of order  $10^{-10}$ , and the magnetic torque is of order 10. Based on our previous work, we furthermore know that the particle-interface interaction force can be of order  $10^{-3}$ .<sup>15</sup> Thus,

we can neglect magnetic dipole-dipole interactions between the particles. Experimentally, the magnetic torque  $Me$  can be of order of the capillary torque  $\gamma_{12}a^2$ . Taking  $a = 10\text{nm}$ , and using the surface tension  $\gamma_{12} \approx 70\text{ mN/m}$  of a water-oil interface, we obtain the magnetic torque  $Me \approx 7 \times 10^{-18}\text{Nm}$ . This torque should be achievable with a strong magnet (*e.g.*,  $H \approx 0.07T$ ) and a magnetic moment of  $1 \times 10^{-16}\text{Nm/T}$ . The resulting magnetic interaction force is of order  $10^{-17}N$ , which is much smaller than the resulting particle-interface interaction force  $\gamma_{12}a$  of order  $10^{-9}N$ .

For a detailed description of the method and our implementation including, we refer the reader to the relevant literature.<sup>12,19,20</sup>

We perform simulations of single and multiple particles in a system containing two fluid components. The system size is  $S = 256 \times 256 \times 144$  and the droplet radius is 100. Particles with radius 20 are used when there are  $N = 1 - 6$  particles in the system, while the radius is lowered to  $a = 10$  for the system containing  $N = 40$  particles.

**Interfacial energy of a single Janus particle at a droplet interface.** When Janus particles are absorbed at the droplet interface, the interface can be deformed due to gravity, rotation, anisotropic shape or surface roughness of the particles. Our lattice Boltzmann simulations are capable of capturing the interface deformations without making any assumptions about the magnitude of the deformations or stipulating any particle-fluid boundary conditions, as shown in our previous work.<sup>12</sup> To develop a theoretical model to describe the behaviour observed in the simulations, we consider particles with a radius much smaller than the capillary length such that we can neglect the effect of gravity. Our particles are spheres, thus we can eliminate the deformation due to an anisotropic shape or a rough surface of the particles.

The interface deformation in our system is mainly induced by the rotation of the particles. However, the difficulty in modelling the shape of the interface and the position of the contact line prevents any exact analytical expression to exist for this problem. Park and Lee<sup>10</sup> numerically calculate the interface deformation introduced by rotation of ellipsoidal and dumbbell Janus particles. They find that the theoretical model that assumes no interface deformation is able to predict the equilibrium orientation of nanoparticles reasonably accurately. Moreover, the interface deformation is highly dependent on the tilt angle of the Janus particle. The tilt angle is defined as the angle between particle orientation and normal direction of the droplet interface. The interface deformation increases with an increasing tilt angle for small tilt angles. In our system, for example, under an upward magnetic field, the particle will move to the top of the droplet, which means the tilt angle of the Janus particle with respect to the normal direction of the droplet interface is zero. Therefore, we propose a theoretical model assuming that interface deformation is negligible.

The interface energy of the particle in its equilibrium

configuration is

$$E_{\text{int}} = \gamma_{12}A_{12}^{\text{int}} + \gamma_{a1}A_{a1}^{\text{int}} + \gamma_{p2}A_{p2}^{\text{int}}, \quad (8)$$

where  $\gamma_{ij}$  are the interface tensions between phases  $i$  and  $j$  and  $A_{ij}$  are the contact surface areas between phases  $i$  and  $j$ , where  $i, j = \{1: \text{fluid}, 2: \text{fluid}, a: \text{apolar}, p: \text{polar}\}$ . Under the assumption that the particle radius is substantially smaller than the droplet radius, the local interface around the Janus particle can be approximated by a flat plane that is tilted with respect to the horizontal direction by an angle  $\phi$ . Thus, the global curvature of the droplet interface has an effect on the interface energy of this system and we can neglect the effect of the local curvature. We then obtain  $A_{12}^{\text{int}} = 2\pi R^2 - \pi a^2$ . In the case of a symmetric amphiphilic spherical particle, the apolar and polar surface areas are equal, *i.e.*,  $A_{a1} = A_{p2} = 2\pi a^2$ .

Under a strong magnetic field, the magnetic dipole will align in parallel to the direction of the magnetic field. At first, we assume the particle's position is fixed, thus the interface energy of a Janus particle can be written as

$$E_{\text{mag}} = \gamma_{12}A_{12}^{\text{mag}} + \gamma_{a1}A_{a1}^{\text{mag}} + \gamma_{p2}A_{p2}^{\text{mag}} + \gamma_{a2}A_{a2} + \gamma_{p1}A_{p1}. \quad (9)$$

where  $A_{12}^{\text{mag}} = 2\pi R^2 - \pi a^2$ .

The interface energy difference between the magnetic field induced orientation state and the initial state is

$$\begin{aligned} \Delta E &= E_{\text{mag}} - E_{\text{int}} \\ &= \gamma_{12}(A_{12}^{\text{mag}} - A_{12}^{\text{int}}) + \gamma_{a1}(A_{a1}^{\text{mag}} - A_{a1}^{\text{int}}) \\ &\quad + \gamma_{p2}(A_{p2}^{\text{mag}} - A_{p2}^{\text{int}}) + \gamma_{a2}A_{a2} + \gamma_{p1}A_{p1}. \end{aligned} \quad (10)$$

Since  $A_{a1}^{\text{int}} = A_{a1}^{\text{mag}} + A_{a2}$  and  $A_{p2}^{\text{int}} = A_{p2}^{\text{mag}} + A_{p1}$ , we obtain

$$\begin{aligned} \Delta E &= \gamma_{12}(A_{12}^{\text{mag}} - A_{12}^{\text{int}}) + (\gamma_{a2} - \gamma_{a1})A_{a2} \\ &\quad + (\gamma_{p1} - \gamma_{p2})A_{p1}, \end{aligned} \quad (11)$$

According to Young's boundary conditions,<sup>41</sup> we obtain

$$\cos \theta_A = \frac{\gamma_{a1} - \gamma_{a2}}{\gamma_{12}}, \quad \cos \theta_P = \frac{\gamma_{p1} - \gamma_{p2}}{\gamma_{12}}. \quad (12)$$

Using  $\cos \theta_A = -\cos \theta_P = -\sin \beta$  resulting from the condition that the two hemispheres have opposite wettabilities, we can further simplify Eq. (11) to

$$\Delta E = \gamma_{12}(A_{12}^{\text{mag}} - A_{12}^{\text{int}}) + \gamma_{12}(A_{a2} + A_{p1}) \sin \beta. \quad (13)$$

Under the assumption that the interface deformation is negligible,  $A_{12}^{\text{mag}} = A_{12}^{\text{int}}$ ,  $A_{a2} = A_{p1} = \frac{\phi}{2\pi}4\pi a^2 = 2\phi a^2$ . Therefore, Eq. (11) finally reduces to

$$\Delta E = 4\phi a^2 \gamma_{12} \sin \beta. \quad (14)$$

**Total interface energy of multiple particles at a droplet interface.** If there are  $N$  particles adsorbed at the interface, the total interface energy becomes

$$\Delta E_T = 4a^2 \gamma_{12} \sin \beta \sum_i^N \phi_i. \quad (15)$$

Based on a geometrical analysis, we get

$$\sin \phi/2 = \frac{|\mathbf{r}_i - \mathbf{r}_0|}{2R}. \quad (16)$$

Under the effect of an upward magnetic field, the particles move to the top, resulting a small  $\phi$  angle. Therefore, we can write

$$\phi/2 \approx \frac{|\mathbf{r}_i - \mathbf{r}_0|}{2R}. \quad (17)$$

Then, we can rewrite Eq. (15) into

$$\Delta E_T = \frac{4a^2\gamma_{12}\sin\beta}{R} \sum_i^N |\mathbf{r}_i - \mathbf{r}_0|. \quad (18)$$

## ACKNOWLEDGMENTS

Financial support is acknowledged from NWO/STW (STW project 13291). We thank the Jülich Supercomputing Centre and the High Performance Computing Center Stuttgart for the technical support and allocated CPU time.

**Supporting Information Available:** Movies visualizing the assembly process of multiple Janus particles are available free of charge *via* the Internet at <http://pubs.acs.org>.

- 
- [1] Boal, A.; Ilhan, F.; De Rouchey, J.; Thurn-Albrecht, T.; Russell, T.; Rotello, V. Self-Assembly of Nanoparticles into Structured Spherical and Network Aggregates. *Nature* **2000**, *404*, 746–748.
  - [2] Olson, M. A.; Coskun, A.; Klajn, R.; Fang, L.; Dey, S. K.; Browne, K. P.; Grzybowski, B. A.; Stoddart, J. F. Assembly of Polygonal Nanoparticle Clusters Directed by Reversible Noncovalent Bonding Interactions. *Nano Lett.* **2009**, *9*, 3185–3190.
  - [3] Hermanson, K. D.; Lumsdon, S. O.; Williams, J. P.; Kaler, E. W.; Velev, O. D. Dielectrophoretic Assembly of Electrically Functional Microwires from Nanoparticle Suspensions. *Science* **2001**, *294*, 1082–1086.
  - [4] Weiss, P. S. Hierarchical Assembly. *ACS Nano* **2008**, *2*, 1085–1087.
  - [5] Grzelczak, M.; Vermant, J.; Furst, E. M.; Liz-Marzán, L. M. Directed Self-Assembly of Nanoparticles. *ACS Nano* **2010**, *4*, 3591–605.
  - [6] Binks, B. P.; Fletcher, P. D. I. Particles adsorbed at the Oil-Water Interface: A Theoretical Comparison between Spheres of Uniform Wettability and “Janus” Particles. *Langmuir* **2001**, *17*, 4708–4710.
  - [7] Lin, Y.; Böker, A.; Skaff, H.; Cookson, D.; Dinsmore, D.; Emrick, T.; Russell, T. P. Nanoparticle Assembly at Fluid Interfaces: Structure and Dynamics. *Langmuir* **2005**, *21*, 191–194.
  - [8] Böker, A.; He, J.; Emrick, T.; Russell, T. P. Self-Assembly of Nanoparticles at Interfaces. *Soft Matter* **2007**, *3*, 1231–1248.
  - [9] Jiang, X.; Zeng, Q.; Chen, C.; Yu, A. Self-Assembly of Particles: Some Thoughts and Comments. *J. Mater. Chem.* **2011**, *21*, 16797–16805.
  - [10] Park, B. J.; Lee, D. Equilibrium Orientation of Nonspherical Janus Particles at Fluid-Fluid Interfaces. *ACS Nano* **2012**, *6*, 782–790.
  - [11] Davies, G. B.; Krüger, T.; Coveney, P. V.; Harting, J.; Bresme, F. Interface Deformations Affect the Orientation Transition of Magnetic Ellipsoidal Particles Adsorbed at Fluid-Fluid Interfaces. *Soft Matter* **2014**, *10*, 6742–6748.
  - [12] Xie, Q.; Davies, G. B.; Günther, F.; Harting, J. Tunable Dipolar Capillary Deformations for Magnetic Janus Particles at Fluid-Fluid Interfaces. *Soft Matter* **2015**, *11*, 3581–3588.
  - [13] Newton, B. J.; Buzza, D. M. A. Magnetic Cylindrical Colloids at Liquid Interfaces Exhibit Non-Volatile Switching of Their Orientation in an External Field. *Soft Matter* **2016**, *12*, 5285–5296.
  - [14] Davies, G. B.; Krüger, T.; Coveney, P. V.; Harting, J.; Bresme, F. Assembling Ellipsoidal Particles at Fluid Interfaces Using Switchable Dipolar Capillary Interactions. *Adv. Mater.* **2014**, *26*, 6715–6719.
  - [15] Xie, Q.; Davies, G. B.; Harting, J. Controlled Capillary Assembly of Magnetic Janus Particles at Fluid-Fluid Interfaces. *Soft Matter* **2016**, *12*, 6566–6574.
  - [16] Cavallaro, M.; Botto, L.; Lewandowski, E. P.; Wang, M.; Stebe, K. J. Curvature-Driven Capillary Migration and Assembly of Rod-Like Particles. *Proc. Natl. Acad. Sci. U. S. A.* **2011**, *108*, 20923–20928.
  - [17] Ershov, D.; Sprakel, J.; Appel, J.; Cohen Stuart, M.; van der Gucht, J. Capillarity-Induced Ordering of Spherical Colloids on an Interface with Anisotropic Curvature. *Proc. Natl. Acad. Sci. U. S. A.* **2013**, *110*, 9220–9224.
  - [18] Hessling, D.; Xie, Q.; Harting, J. Diffusion Dominated Evaporation in Multicomponent Lattice Boltzmann Simulations. *J. Chem. Phys.* **2017**, *146*, 054111.
  - [19] Jansen, F.; Harting, J. From Bijels to Pickering Emulsions: A Lattice Boltzmann Study. *Phys. Rev. E* **2011**, *83*, 046707.
  - [20] Frijters, S.; Günther, F.; Harting, J. Effects of Nanoparticles and Surfactant on Droplets in Shear Flow. *Soft Matter* **2012**, *8*, 6542–6556.
  - [21] Krüger, T.; Frijters, S.; Günther, F.; Kaoui, B.; Harting, J. Numerical Simulations of Complex Fluid-Fluid Interface Dynamics. *Eur. Phys. J.: Spec. Top.* **2013**, *222*, 177–198.
  - [22] Duan, H.; Wang, D.; Kurth, D. G.; Möhwald, H. Directing Self-Assembly of Nanoparticles at Water/Oil Interfaces. *Angew. Chem., Int. Ed.* **2004**, *43*, 5639–5642.
  - [23] Lu, J.; Aabdin, Z.; Loh, N. D.; Bhattacharya, D.; Mirsaidov, U. Nanoparticle Dynamics in a Nanodroplet. *Nano Lett.* **2014**, *14*, 2111–2115.
  - [24] Bai, P.; Hayes, R.; Jin, M.; Shui, L.; Chuan Yi, Z.; Wang, L.; Zhang, X.; Zhou, G. F. Review of Paper-Like Display Technologies. *Prog. Electromagn. Res.* **2014**, *147*, 95–116.
  - [25] Lohse, D.; Zhang, X. Surface Nanobubbles and Nanodroplets. *Rev. Mod. Phys.* **2015**, *87*, 981–1035.
  - [26] Yu, H.; Maheshwari, S.; Zhu, J.; Lohse, D.; Zhang, X.



- Formation of Surface Nanodroplets Facing a Structured Microchannel Wall. *Lab Chip* **2017**, *17*, 1496–1504.
- [27] Rahimi, M.; Roberts, T. F.; Armas-Pérez, J. C.; Wang, X.; Bukusoglu, E.; Abbott, N. L.; de Pablo, J. J. Nanoparticle Self-Assembly at the Interface of Liquid Crystal Droplets. *Proc. Natl. Acad. Sci. U. S. A.* **2015**, *112*, 5297–5302.
- [28] Pine, D. J. Dense Packing and Symmetry in Small Clusters of Microspheres. *Science* **2003**, *30*, 483–487.
- [29] Arkus, N.; Manoharan, V. N.; Brenner, M. P. Minimal Energy Clusters of Hard Spheres with Short Range Attractions. *Phys. Rev. Lett.* **2009**, *103*, 118303.
- [30] Comiskey, B.; Albert, J. D.; Yoshizawa, H.; Jacobson, J. An Electrophoretic Ink for All-Printed Reflective Electronic Displays. *Nature* **1998**, *394*, 253–255.
- [31] Succi, S. *The Lattice Boltzmann Equation for Fluid Dynamics and Beyond*; Oxford University Press, 2001.
- [32] Shan, X.; Chen, H. Lattice Boltzmann Model for Simulating Flows with Multiple Phases and Components. *Phys. Rev. E* **1993**, *47*, 1815.
- [33] Liu, H.; Kang, Q.; Leonardi, C. R.; Schmieschek, S.; Narvaez Salazar, A.; Jones, B. D.; Williams, J. R.; Valocchi, A. J.; Harting, J. Multiphase Lattice Boltzmann Simulations for Porous Media Applications - A Review. *Computat. Geosci.* **2016**, *20*, 777–805.
- [34] Ladd, A. J. C.; Verberg, R. Lattice-Boltzmann Simulations of Particle-Fluid Suspensions. *J. Stat. Phys.* **2001**, *104*, 1191–1251.
- [35] Bhatnagar, P.; Gross, E.; Krook, M. A Model for Collision Processes in Gases. I. Small Amplitude Processes in Charged and Neutral One-Component Systems. *Phys. Rev.* **1954**, *94*, 511.
- [36] Chen, H.; Chen, S.; Matthaeus, W. H. Recovery of the Navier-Stokes Equations Using a Lattice-Gas Boltzmann Method. *Phys. Rev. A* **1992**, *45*, R5339.
- [37] Huang, H.; Thorne, D. T.; Schaap, M. G.; Sukop, M. C. Proposed Approximation for Contact Angles in Shan-and-Chen-Type Multicomponent Multiphase Lattice Boltzmann Models. *Phys. Rev. E* **2007**, *76*, 066701.
- [38] Aidun, C. K.; Lu, Y.; Ding, E.-J. Direct Analysis of Particulate Suspensions with Inertia Using the Discrete Boltzmann Equation. *J. Fluid Mech.* **1998**, *373*, 287–311.
- [39] Stratford, K.; Adhikari, R.; Pagonabarraga, I.; Desplat, J.-C.; Cates, M. E. Colloidal Jamming at Interfaces: A Route to Fluid-Bicontinuous Gels. *Science* **2005**, *309*, 2198–2201.
- [40] Joshi, A. S.; Sun, Y. Multiphase Lattice Boltzmann Method for Particle Suspensions. *Phys. Rev. E* **2009**, *79*, 066703.
- [41] Ondarçuhu, T.; Fabre, P.; Raphaël, E.; Veyssié, M. Specific Properties of Amphiphilic Particles at Fluid Interfaces. *J. Phys.* **1990**, *51*, 1527–1536.